electronics

Article

EV-Station-Grid Coordination Optimization Strategy Considering Psychological Preferences

Chudi Wang *, Shaohua Ma *, Qiwei Wang, Ning Yan, Yannan Dong and Zhiyuan Cai

Department of Electrical Engineering, Shenyang University of Technology, Shenyang 110870, China
* Correspondence: wcd583455822@126.com (C.W.); mash_dq@sut.edu.cn (S.M.)

Abstract: This paper proposes the electric vehicle (EV)-station-grid coordination optimization strategy considering user preferences, which regulates the charging behaviors of EV users from the user side to ensure the stable and safe operation of the power grid. Firstly, the spatio-temporal prediction model of charging load based on speed-temperature is developed. The model of EV power consumption per unit mileage affected by temperature and EV speed is constructed, and the shortest path algorithm is applied to determine the driving paths of EVs so as to judge the charging demand in combination with the state of charge (SOC) of the battery and to determine the charging periods and locations of the EVs, thus obtaining the spatio-temporal information of the charging load. Secondly, a multi-attribute charging decision model considering user preferences is constructed. Fuzzy clustering and rough set theory are applied to mine user behavior preferences, combined with behavioral economics to describe users' irrational charging decision-making psychology. Lastly, a real-time charging price model considering voltage fluctuation index and user charging cost is constructed to analyze the impact of price on guiding charging behaviors. The simulation results verify the effectiveness and performance of the collaborative optimization strategy.

Keywords: electric vehicle; coordination optimization strategy; preference mining; behavioral economics; road-grid coupling network

Citation: Wang, C.; Ma, S.; Wang, Q.; Yan, N.; Dong, Y.; Cai, Z. EV-Station-Grid Coordination Optimization Strategy Considering Psychological Preferences. *Electronics* **2023**, *12*, 1935. https://doi.org/10.3390/electronics12081935

Academic Editors: Danial Karimi and Amin Hajizadeh

Received: 16 March 2023
Revised: 13 April 2023
Accepted: 14 April 2023
Published: 20 April 2023

1. Introduction

As a flexible resource on the load side, the electric vehicle (EV) is not only conducive to the construction of new power systems but also an important tool to achieve the target of "Carbon Emission Peak and Carbon Neutrality" [1]. However, with the continuous improvement in the popularity of EVs, the extensive access of EVs also brings new challenges to the stable operation of existing systems. On the one hand, the charging load of EVs is affected by the heterogeneity of users' travel. The charging load of EVs has unique temporal and spatial randomness [2,3], which makes it more difficult to mine the charging laws. On the other hand, restricted by the layout and configuration of existing charging facilities, when large-scale EVs are connected to the power grid, their charging demand is difficult to be fully met, resulting in excessive load fluctuation, deteriorating the power quality and even endangering the security of supply and other problems [4,5].

Until now, there have been a number of studies on guiding users to charge in an orderly manner. In [6], the algorithm provides a load leveling or peak shaving service by managing the current absorbed by each electrical bus in a charging station, while satisfying the charging requirements of electric buses and adhering to a reasonable connection pattern defined by the fleet limit of electric buses. Literature [7] investigates a coordinated charging where EVs are charged via an "aggregator" that interacts with a power system operator to schedule EV charging at times that either minimize system operating costs, decrease EV charging costs, or both, while meeting the daily EV charging requirements subject to the EV owners' charging constraints. Beta distributions were found to be the most appropriate distribution for statistically modeling the initial and final state of charge of vehicles in an EV fleet. Literature [8] proposes an optimization model based on time-of-use (TOU) price, which realizes the effect of orderly charging on peak load shifting. In [9], a novel prioritization-based load management method was developed to prevent loss of comfort and increase in consumption cost caused by the conventional load management approximations based on static priority. A house that has four MLs such as air conditioner (AC), water heater (WH), clothes dryer (CD), and EV in the case study shows the performance of the proposed methods within a two-day simulation. Game theory can effectively solve the problem of how to reasonably set the charging price while protecting the interests of multiple parties. Literature [10] proposes a large-scale EV real-time scheduling model based on dynamic non-cooperative game, which considers the interests of multiple electric vehicle aggregators (EVA). The proposed model can effectively reduce load fluctuation as well as the cost of EVA charging. Literature [11] proposed a demand response algorithm to optimize vehicle to grid (V2G) aggregation by enabling EVs scheduled charging/discharging in a quest to minimize the energy cost for the retailer, as well as satisfying the electricity market, i.e., day-ahead and instantaneous real-time markets. Where the consumers' contribution has been modeled as correlative game, each consumer is taking part as a player and tends to enhance his own incentives payoff (profit) by using the techniques proposed in this paper. Literature [12] studies the problem of energy charging using a robust Stackelberg game approach in a power system composed of an aggregator and multiple electric vehicles (EVs) in the presence of demand uncertainty and proposes two different robust approaches: a non-cooperative optimization and a co-operative design. The effectiveness of the robust solutions in uncertain environments is verified. The above studies have realized the effect of orderly charging on peak load shifting or the economic benefits of users by adjusting charging prices. However, the strategy of the above research on charging behavior is mainly focused on the time dimension, without taking into account the guidance role of the space dimension; thus, the imbalance of the overall regional charging load distribution has not been resolved.

The charging load has the dual attributes of road network and power grid, so the charging optimization strategy architecture under the EV-station-grid cooperation mode can effectively solve the problem of unbalanced regional charging load distribution. In [13], a load transfer scheme between transmission and distribution networks is proposed, which can effectively provide a reference for power grid dispatchers and improve the security and economy of the power system. In [14], the driving behaviors of EVs are simulated by the microscopic traffic flow model, and then, a bi-level dynamic charging scheduling model is presented with objectives of optimally tracking the day-ahead scheduling and minimizing the waiting time cost of EVs. In [15], the charging price model is established based on the dynamic price demand function under the constraint of dynamic queue and node voltage so as to guide users to select fast charging stations with the goal of minimum charging cost.

The strategies constructed in the above literature take into account the objective factors such as traffic flow, time, price, etc. to parallelly guide the charging load in the time and space, achieving the targets of alleviating the regional load imbalance and improving the power quality of the distribution network. However, there is a basic assumption in the above strategies—the decision maker is completely rational when making the charging choice behavior [16], without considering the impact of subjective psychology on the decision. EV users are faced with a multi-dimensional, dynamic, and uncertain environment with mutual influence between strategies when making charging decisions. It is difficult for decision makers to obtain sufficient information and make accurate predictions of the situation. In this case, users often obtain information by observing the behavior from others, resulting in irrational behaviors such as herding effect [17] and endowment effect [18]. In addition, the charging decision-making group has a large scale and a wide distribution of members. The decision-making attributes present complexity and randomness, manifested in the existence of multiple dimensions of evaluation attributes in decision-making issues, and the importance of these attributes is different. That is, users tend to pay more attention to the changes of some attributes when making decisions, while being relatively insensitive to other attributes, presenting unique psychological preferences. Literature [19] uses the quantitative product between the preference vectors between two decision members to illustrate the relationship between the corresponding two decision members and uses similarity relationships to divide decision members into the same aggregation. Literature [20] synthesizes each attribute weight vector and a large group preference matrix and determines the ranking of decision-making options based on the comprehensive evaluation vector of each option. Literature [21] proposes a large group decision-making method oriented to utility value preference information. However, the above multiple attribute decision making problems do not take into account the irrational psychology of decision makers in the process of preference mining. By analyzing the advantages and disadvantages of the above methods, this paper proposes an irrational group decision-making method that considers complex preferences, and the established model is more consistent with the actual decision-making process.

Based on the above, this paper proposes the EV-station-grid coordination optimization strategy considering user preferences, describing irrational psychology through prospect theory [22], mining user preferences through clustering, establishing a multi-objective optimization model to regulate the spatial and temporal distribution of charging loads, achieving the goal of peak shaving and valley filling, and reducing grid fluctuations. Users can also effectively reduce charging costs by responding to the optimization objectives, while charging station operators can ensure profitability by regulating prices.

The method proposed in this article breaks the assumption of rational decision-making principles and broadens the application scope of behavioral economics, improving the accuracy of decision model results from the very beginning, and collaborative optimization strategy provides theoretical support for formulating scientific charging guidance schemes. The contributions of this paper can be summarized as follows:

1. The charging decision model based on the prospect theory is proposed, and user behavior preferences are mined by combining fuzzy clustering and rough set theory [23–25]. The diversity of decision makers' behavior preferences, multi-dimension of decision factors, and time variant of decision objectives are fully considered.
2. The model of EV power consumption per unit mileage based on speed-flow practical model is constructed. The shortest path algorithm [26] is used to determine the EV's driving path, and the charging demand is judged in combination with the state of charge (SOC) of the battery under the influence of temperature so as to obtain the spatiotemporal information of the charging load.
3. A bi-level collaborative optimization strategy is proposed to guide users to charge in an orderly manner by formulating a real-time charging price not only to improve the power quality of the grid and reduce the comprehensive charging cost of users but also to ensure the basic profit of the charging station operator, thus achieving a better interaction between the EV, station, and grid.

The rest of this article is arranged as follows. In Section 2, the spatio-temporal prediction of charging load considering speed–temperature is proposed. In Section 3, prospect theory, fuzzy clustering, and rough set theory are combined to propose an irrational charging decision model considering user preferences. In Section 4, a bi-level collaborative optimization strategy based on real-time charging price is proposed to guide users' charging behavior with the goal of reducing grid fluctuation index and reducing user costs. Section 5 is example analysis, and the last section is the conclusion.

2. Spatio-Temporal Prediction of Charging Load

2.1. Construction of Physical Road Network

The physical road network carries various road weight distribution and traffic rules. This paper abstracts the physical road network with the geometric centerline of the road and describes and explains the topological structure of the road network with the graph theory [27].

$$\begin{cases} \epsilon = (N_\epsilon, E_\epsilon, \delta_\epsilon) \\ N_\epsilon = \{n_i | i = 1, 2, \ldots, u\} \\ E_\epsilon = \{\langle n_i, n_j \rangle | n_i, n_j \in N\} \\ \delta_\epsilon = \{e_{ij} | \langle n_i, n_j \rangle \in E\} \end{cases} \tag{1}$$

where ϵ represents the road network topology, which is composed of N_ϵ, E_ϵ, and δ_ϵ.N_ϵ is the intersection node in the road network; that is, the road intersection set, u, is the total number of nodes, and E_ϵ is the road segment set in the road network. δ_ϵ is the adjacency matrix of the road weight value, describing the length of each road section and the connection relationship of nodes, and the length of the road e_{ij} is determined according to Formula (2).

$$e_{ij} = \begin{cases} d_{ij}, i \text{ is connected with } j \\ 0, \qquad\qquad i = j \\ \inf, i \text{ is not connecte dwith } j \end{cases} \tag{2}$$

where inf means infinite, d_{ij} is the distance of road $\langle n_i, n_j \rangle$, and $d_{ij} \neq 0$.

2.2. Practical Speed–Flow Relationship Model

Travel time is one of the important factors affecting the charging decision of users. In the condition that the road length is known, the travel time is determined by the driving speed, which is affected by the road capacity and traffic flow. EV driving speed directly affects the power consumption per unit mileage and then affects the charging demand of EV users. Therefore, this paper introduces the practical speed–flow relationship model to calculate the real-time driving speed of EVs $v_{ij}(t)$.

$$\begin{cases} v_{ij}(t) = \frac{v_{ij,m}}{1+(Q_{ij}(t)/\rho_{ij})^\beta} \\ \beta = a + b(Q_{ij}(t)/\rho_{ij})^\gamma \end{cases} \tag{3}$$

where $v_{ij,m}$ represents the zero flow velocity of road $E(i,j)$; ρ_{ij} is the capacity of road $E(i,j)$, which is proportional to the road grade; $Q_{ij}(t)$ is the traffic flow of road $E(i,j)$ at time t; the ratio of $Q_{ij}(t)$ to ρ_{ij} is the road saturation at time t; β is the empirical coefficient; a,b,γ is the adaptive coefficient under different roads and the phase angle difference of the branch ij levels.

2.3. Influence of Temperature on Charging Demand

2.3.1. Effect of Temperature on Battery Performance

Most of the power batteries of EVs are lithium iron phosphate batteries, which are sensitive to temperature. The capacity of the battery at different temperatures was analyzed in literature [28]. Taking the discharge capacity of 25 °C as the reference point for the performance test, the change curve of battery capacity is relatively obvious at the low temperature stage. At 0 °C, the battery capacity is 79.3% of the normal capacity. When the temperature drops to below 0 °C, the performance of the battery decreases due to the low temperature environment, which makes the discharge capacity of the battery decline faster. At −20 °C, the relative capacity of the battery is only 43.6%, while at the high temperature stage, the battery capacity change curve is not obvious.

2.3.2. Influence of Temperature on Air-Conditioner (AC) System Energy Consumption

The AC system in EVs is the highest energy-consuming equipment second only to the motor. Literature [29] investigated the probability of EV owners starting the AC system under different temperatures and found the probability conforms to the normal distribution, as shown in Figure 1.

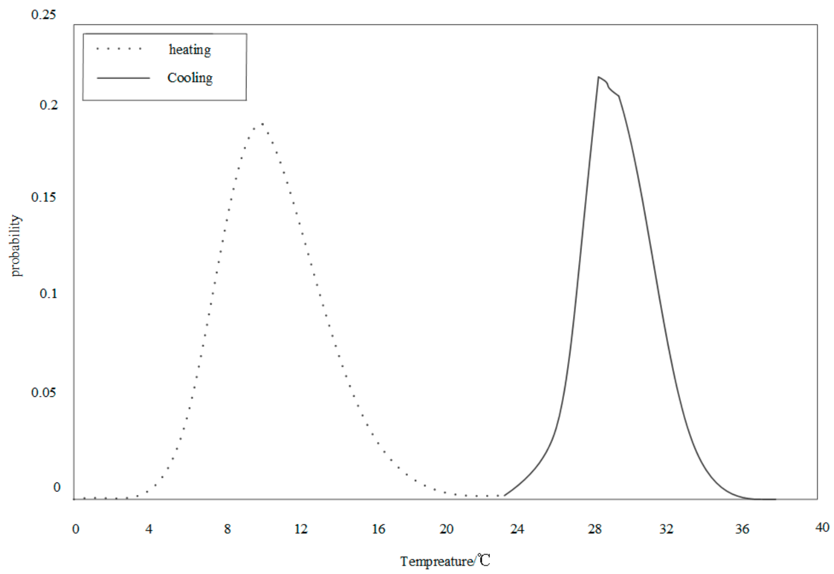

Figure 1. Probability distribution of AC system start.

The heating temperature threshold and the cooling temperature threshold are around 11 °C and 30 °C, respectively. Thus, the probability density function of AC startup is

$$(Tem) = \frac{1}{\sqrt{2\pi}\delta_{Tem}} \exp\left[-\frac{(Tem - u_{Tem})^2}{2(\delta_{Tem})^2}\right] \tag{4}$$

where, in the case of heating startup, u_{Tem}= 10.82, δ_{Tem} = 2.14, and in the case of cooling startup, u_{Tem}= 29.4, δ_{Tem} = 1.75.

2.3.3. SOC Analysis of EVs Considering Temperature

Temperature can affect the energy consumption per unit mileage of EVs by influencing additional energy consumption, battery performance, road conditions, and other factors. The energy consumption factor in literature [29] is used to describe the EV battery power consumption per unit mileage, and the regression model is used to establish the power consumption model per unit mileage at a certain speed.

$$ECF = a/v(t) + bv(t) + cv(t)^2 + d \tag{5}$$

where *ECF* is the power consumption factor, and $v(t)$ is the speed of EVs on road *E*(*i*,*j*) at time *t*. *a*, *b*, *c*, *d* are the fitting coefficients, which are different under various road grades.

Thus, the driving power consumption SOC_i^t of EV *i* at time *t* can be obtained.

$$SOC_i^t = ECF \times L(t) \tag{6}$$

where $L(t)$ is the mileage driven by EV at time *t*.

Temperature determines the working performance of the battery to some extent. Taking 25 °C as the reference basis, the actual capacity of the battery at different temperatures can be obtained:

$$D(T) = \mu \cdot D(25) \tag{7}$$

where $D(T)$ represents the actual capacity of the battery at T°C, μ is the relative capacity percentage of the battery, and $D(25)$ represents the battery capacity at 25 °C.

Considering the influence of temperature on AC system consumption, it is concluded that the AC system consumption of EVs at different temperatures is as follows:

$$A(T) = \frac{SOC_i^t}{1-\theta}\theta \tag{8}$$

where θ indicates the proportion of AC system consumption, and the refrigeration power consumption of AC accounts for 32.5% of the total power consumption according to literature [30], while the heating power consumption accounts for 35%. When the temperature does not need to open AC, this item is 0. Then, the remaining SOC of the EV i can be expressed as

$$SOC_i^{re} = D(T) - SOC_i^t - A(T) \tag{9}$$

2.3.4. Prediction Framework of EV Charging Load

The spatio-temporal prediction framework of EV charging load considering velocity and temperature proposed in this paper is shown in Figure 2. The framework is based on the road network topology information and traffic information to build the practical speed–flow relationship model. On this basis, the travel information of EVs is generated by the Monte Carlo method, and the energy consumption factor per unit mileage and the proportion of AC power consumption are constructed based on the temperature data and speed data, combined with the shortest distance algorithm, to determine the EV path. Thus, the real-time EV SOC can be analyzed to judge the charging demand.

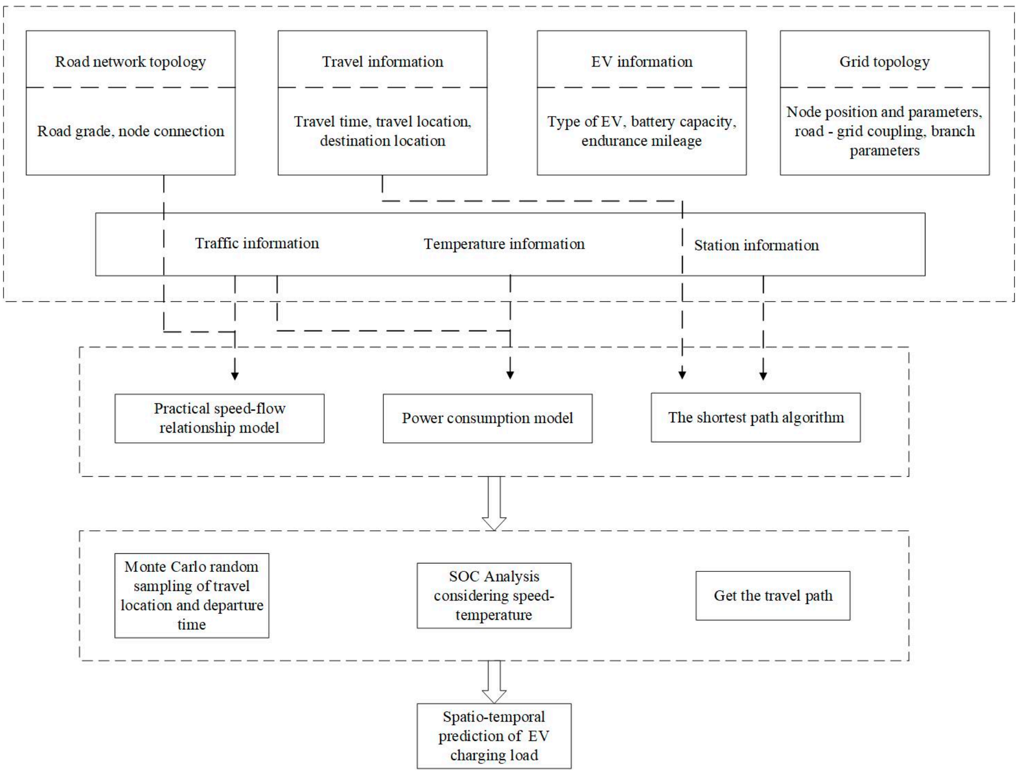

Figure 2. Spatio-temporal prediction framework of charging load considering velocity and temperature.

3. Irrational Charging Decision Model

The framework of the irrational multi-attribute charging decision model considering user preferences is shown in Figure 3. Based on the prospect theory of "irrational people" in the field of behavioral economics, this paper constructs a multi-attribute charging decision model. Charging users need to weigh different decision attributes in multiple candidate schemes and first solve the model from each single attribute index to obtain its corresponding prospect value. Then, the prospect values are aggregated according to the weight; thus, the comprehensive prospect value under multiple attributes of each alternative is obtained. The historical charging data are mined, and the fuzzy clustering and rough set theory are combined to grasp the group preference so as to provide a basis for quantitative research on charging decision-making.

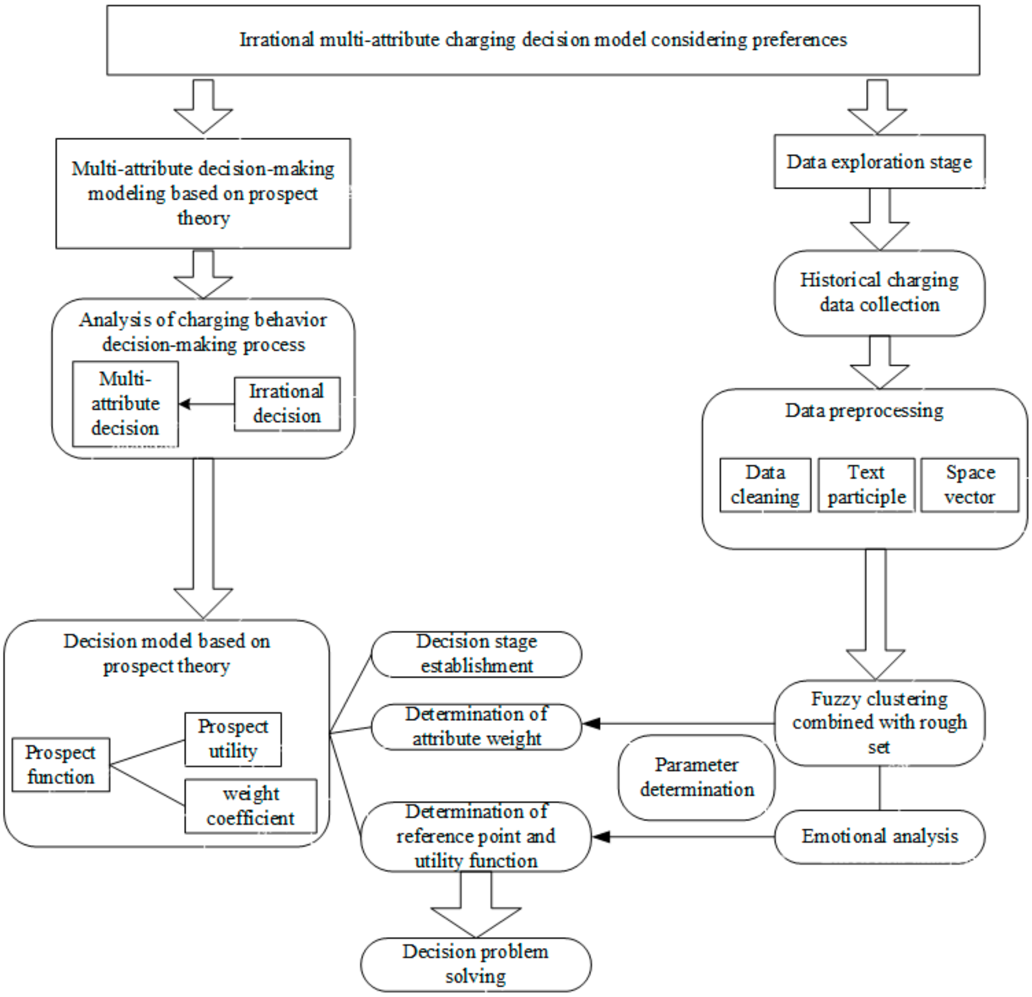

Figure 3. The framework of irrational multi-attribute charging decision model considering preferences.

3.1. Multi-Attribute Charging Decision Model

3.1.1. Prospect Value Function

In prospect theory, which assumes "irrational man", "prospect" is the basic research unit. In the charging decision process, charging costs corresponding to different stations selected by decision makers are "prospects", and users make decisions based on these prospects. However, prospect theory is concerned not with the final state of gain or loss but with the gain or loss relative to the reference point. When an individual is faced with the problem of charging decision, the time and money he pays are all payment items. If the time or cost exceeds the reference value, the excess part can be regarded as a loss. The profit value function $g(x)^+$ and loss value function $g(x)^-$ are shown as follows:

$$G(\Delta x) = \begin{cases} g(x)^+ = (x_r - x)^\alpha, \; x \le x_r \\ g(x)^- = -\lambda(x - x_r)^\beta, \; x > x_r \end{cases} \tag{10}$$

where α is the marginal sensitivity decline coefficient for income; β is the marginal sensitivity decline coefficient for loss; x_r is the reference point; λ represents the loss aversion parameter; and $\lambda > 1$ indicates that individuals are more sensitive to loss.

The study pointed out that when decision makers cannot obtain direct evaluation criteria, they often evaluate themselves by comparing them with others [31]. Therefore, in this paper, 15 min is taken as the time period, and the average value of attributes in the *i*-th period is taken as the reference point for the *i*-th+1 period and updates it so as to provide reference standards for charging users, which is more in line with the "Herd effect" mentality of users.

3.1.2. Utility Integration

When the individual is faced with a multi-attribute decision-making problem, the decision makers will take the budget as the constraint, comprehensively evaluate the loss and gain of each option involved in the decision-making problem relative to the reference point, and integrate to form "transaction utility". Relevant research [32] summarizes four possible methods for individuals to integrate multi-attribute income or loss to form trading utility, which are as follows:

(1) Segregation mode, which is $G(\Delta x) + G(\Delta y) > G(\Delta x + \Delta y)$, $U = G(\Delta x) + G(\Delta y)$.
(2) Loss consolidation mode, which is $G[(-\Delta x) + (-\Delta y)] > G(-\Delta x) + G(-\Delta y)$, $U = G[(-\Delta x) + (-\Delta y)]$.
(3) Integrate smaller losses into larger gains, which is $G[(\Delta x + (-\Delta y)] > G(\Delta x) + G(-\Delta y)$ and $G(\Delta x) > |G(-\Delta y)|$,$U = G[(\Delta x) + (-\Delta y)]$.
(4) When the size of gains and losses cannot be judged, the decision makers may use (1) or (2).

Charging decision involves different attributes relative to its reference points, which may be income or loss. Therefore, this paper assumes that decision makers will adopt the method (a) to integrate multi-attribute gains or losses to form transaction utility, and considering the impact of different types of attribute gains or losses on transaction utility at the same time, the transaction utility function is expressed as $U = \varphi G(\Delta x) + \vartheta G(\Delta y)$.

In this paper, sensitivity analysis is used to determine the sensitivity of decision makers to different factors to analyze the guiding effect of each factor input on charging behavior. Sensitivity is defined as the percentage of change in the value of the objective function caused by a change in an input parameter; that is $R_x = \Delta R_x / R \times 100\%$. Based on the discussion of relevant factors affecting charging decisions in the relevant literature [33–35], sensitivity analysis is conducted by selecting price, time, and battery capacity attributes, as shown in Figure 4a–c.

For every 10% change in the cost, time, and the battery capacity factors, the fitness value changes to 4.336%, 7.901%, and 0.721%. Therefore, it can be concluded that changes in price and time can have an impact on users' charging decisions. Thus, the attributes can be summed up to price attribute—charging price C, and time attribute—travel time T, which is the time of EV driving to the station, and the queuing time T', which is the time from arrival at the charging station to start charging. The collection of charging stations in the area is $R_m = \{1, 2, \ldots i, \ldots, m\}$; accordingly, the utility function after integrating different dimension attributes when charging user n selects charging station i is expressed as

$$U_{ni} = \varphi_{ni}^1 \cdot G_{ni}(\Delta C) + \varphi_{ni}^2 \cdot G_{ni}(\Delta T) + \varphi_{ni}^3 \cdot G_{ni}(\Delta T'),\ i \in R_m \tag{11}$$

where $G_{ni}(\Delta C)$ represents the value function of cost attribute C of station i, while $G_{ni}(\Delta T)$ and $G_{ni}(\Delta T')$ represent the value function of time attributes T and T'; φ_{ni}^1, φ_{ni}^2, and φ_{ni}^3 represent the weights of three attributes, separately.

In this paper, value of time (*vot*) is introduced to transform time and cost so as to realize the effective integration of multi- attribute gain and loss. *Vot* value is the ratio of the average annual salary N_{salary} of EV users to the average annual working hours T_{worktime}.

$$\text{vot} = N_{salary} / T_{worktime} \tag{12}$$

$$\$G(\Delta T) = \begin{cases} vot \times (T_r - T)^{\alpha},\ (T \le T_r) \\ -\lambda vot \times (T - T_r)^{\beta},\ (T > T_r) \end{cases} \tag{13}$$

Finally, the utility function can be expressed as

$$U_{ni} = \varphi_{ni}^{1} \cdot G_{ni}(\Delta C) + \varphi_{ni}^{2} \cdot \$G_{ni}(\Delta T) + \varphi_{ni}^{3} \cdot \$G_{ni}(\Delta T'),\ i \in R_m \tag{14}$$

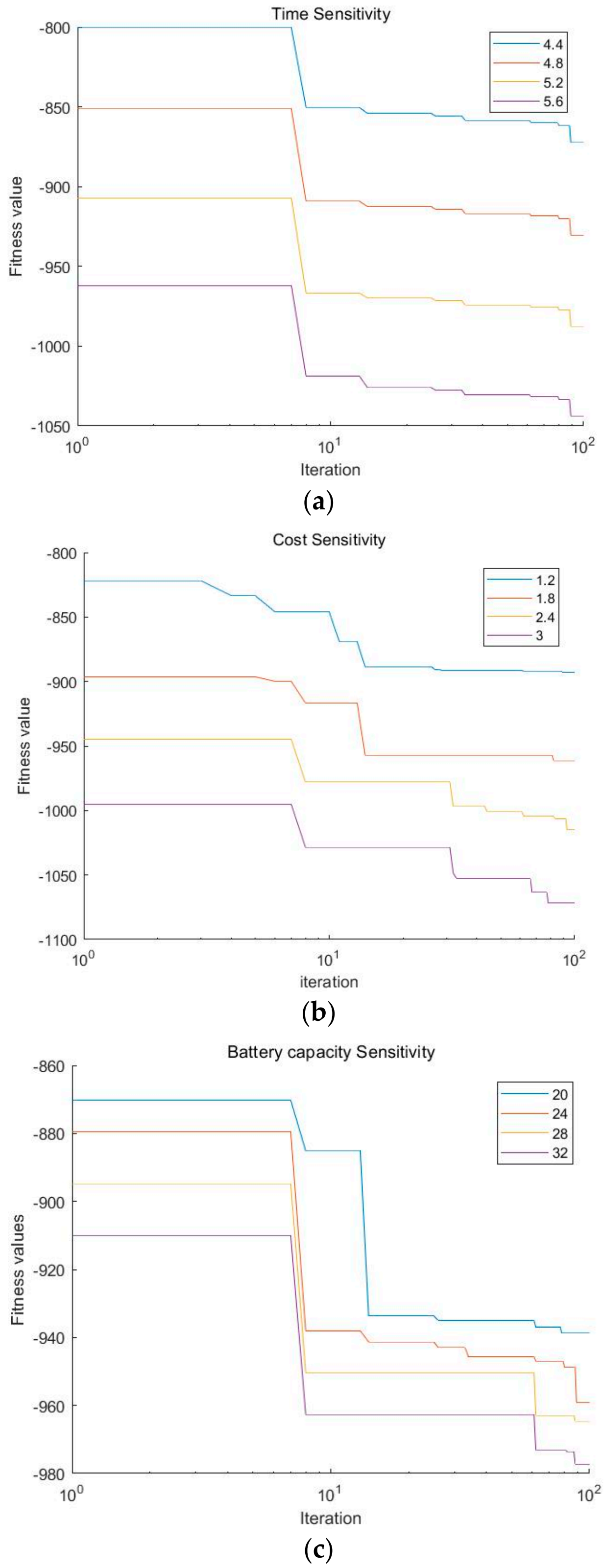

(**a**) (**b**) (**c**)

Figure 4. (**a**) Sensitivity analysis of time; (**b**) Sensitivity analysis of cost; (**c**) Sensitivity analysis of battery capacity.

Therefore, the process of selecting the charging station is actually to compare the weighted attribute values of each selected limb. However, the setting of attribute weight is usually a simple artificial assignment or an assumption that the weight is the same currently. In fact, different attributes must have various influence extents on the decisions, which also leads to the price incentive effect under the unweighted preference not reaching the expectation. Therefore, this paper starts with the user's historical behavior to optimize the attribute weight coefficient and build a multi-attribute charging decision model with behavior preference.

3.2. Behavior Preference Mining

When users make charging decisions, each attribute has a different proportion of influence on charging behavior. However, most of current decision-making models implicitly assume that the contribution of each dimension attribute to decision is the same [36,37] and do not consider the different impacts of each attribute on the decision results, so accurate decision results cannot be obtained. However, groups have the ability to learn and evolve. Therefore, aiming at large complex charging groups, this paper uses fuzzy clustering combined with relative positive domain theory in rough set theory to objectively and indirectly determine the attribute weight of group members' preference vector. This method is suitable for mining preference vector which only has users' historical attribute data and has no prior information of attribute weight assignment by experts. The decision-making process with behavior preferences is shown in Figure 5.

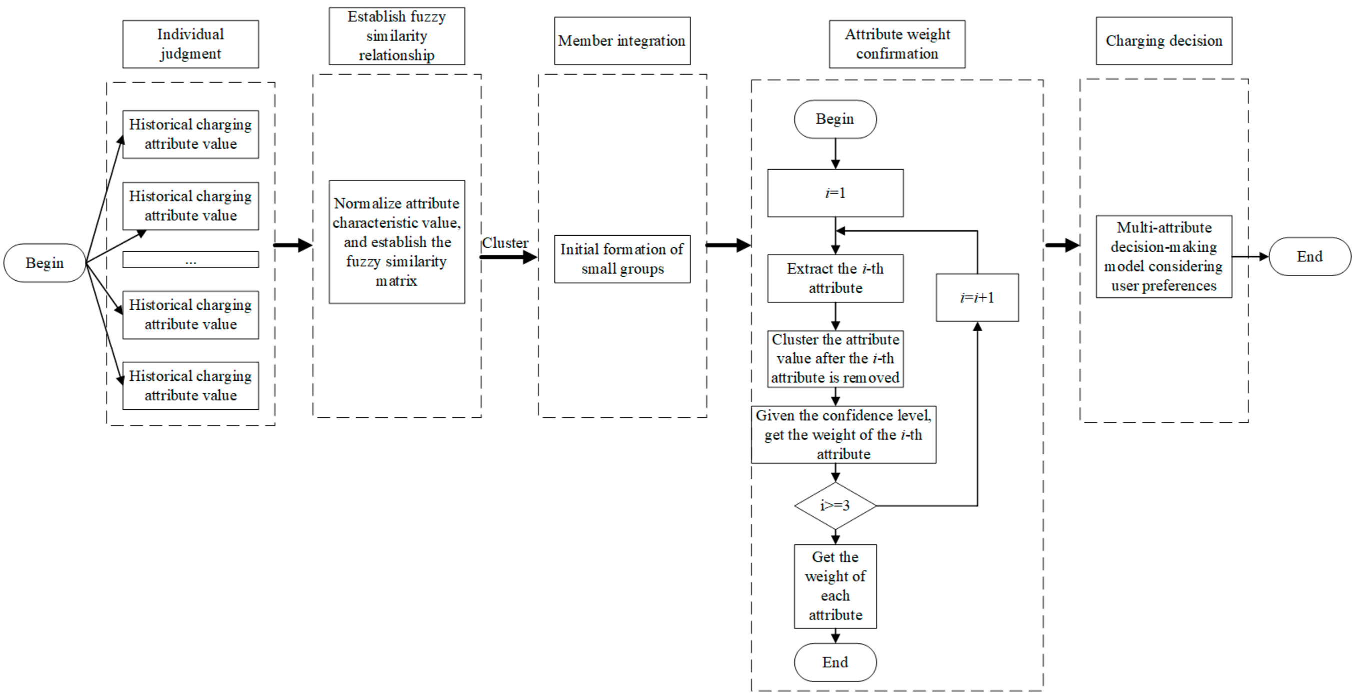

Figure 5. Decision-making process with behavior preferences.

1. Determine the sample objects to be processed. Compose n samples to be processed into a set X:

$$X = \{x_1, x_2, \ldots, x_n\} \tag{15}$$

Each sample is represented by m attribute eigenvalues vectors:

$$X_j = \{x_{1j}, x_{2j}, \ \ldots, \ x_{mj}\} \tag{16}$$

The attributes selected in this paper are respectively C, T, T', then m = 3, and the attribute set can be expressed as

$$X = \left\{ \begin{matrix} x_{11} & x_{12} & \dots & x_{1n} \\ x_{21} & x_{22} & \dots & x_{2n} \\ \vdots & \vdots & \ddots & \vdots \\ x_{m1} & x_{m2} & \dots & x_{mn} \end{matrix} \right\} = \left\{ \begin{matrix} C_1 & C_2 & \dots & C_n \\ T_1 & T_2 & \dots & T_n \\ T_1' & T_2' & \dots & T_n' \end{matrix} \right\} \tag{17}$$

2. Establish fuzzy similarity relationship. Firstly, the attribute characteristic value is normalized to the range [0, 1]. Then, the fuzzy similarity matrix is established, as shown in (17).

$$r_{ij} = \frac{\sum_{k=1}^{m} (x_{ki} \cap x_{kj})}{\sum_{k=1}^{m} (x_{ki} \cup x_{kj})} \tag{18}$$

3. Cluster. The fuzzy equivalent matrix is obtained by the fuzzy equivalent closure method, and then the number of clusters is determined according to the fuzzy equivalent matrix:
   (1) Firstly, the appropriate threshold range is determined according to the fuzzy equivalent matrix. When the cluster is carried out within each threshold range, the lower limit of the threshold range F_k is taken as the mark to record the names and numbers of tuples contained in the categories with different threshold ranges, denoted as $S_i(i = 1{,}2, \dots, k)$.
   (2) According to the definition of attribute importance in the rough set, each attribute is deleted from all attributes in turn, and then, the weight distribution methods 2 and 3 are performed. In the repeated step, the number of clusters is subject to the threshold range determined in step 1, wherein, after deleting each attribute, the entire set is still classified according to the corresponding threshold range. Record the name and number of tuples contained in each cluster, denoted as $S_j'(j = 1{,}2, \dots, k)$, to examine the influence of each attribute on the cluster.
4. Determine the importance of each attribute. Take the classification without deleting any attribute as the benchmark and regard it as a knowledge classification, and the deletion of each attribute is regarded as another kind of knowledge classification. The positive domain of the classification after deletion of each attribute relative to the total attributes classification is analyzed. It is essentially a collection of objects whose classification with one attribute removed can be accurately divided into categories with no attribute removed. It can be seen from the definition of relative positive domain that the relative positive domain of any knowledge is the whole domain relative to itself. According to the particularity of this paper, when all the data are in the same class, or each object is in the same class, the processing method of relative positive domain cannot bring any information. Therefore, these two special cases should be excluded when determining the relative positive domain of each data in this paper. Therefore, at a certain confidence level F_k, the importance of the attribute r can be expressed as follows:

$$\vartheta_{SX'F_k}(S_r) = 1 - \gamma_{s-s'}(X') \tag{19}$$

where S is each conditional attribute investigated in this paper, and X' is the decision attribute set of the attribute r and is the fuzzy clustering indicator of the sample to be investigated.

$\gamma_{s-s'}(X')$ represents the importance of the s'.

Considering that different threshold levels are also different confidence levels in fuzzy clustering, p confidence levels F_k are combined to consider the comprehensive importance of each attribute as

$$\vartheta(S_r) = \left(\sum_{i=1}^{p} F_k \times \vartheta_{SX'F_k}(S_r) \right) / n \tag{20}$$

Thus, the weight distribution of each attribute is determined according to the comprehensive importance:

$$\vartheta'_r = \vartheta(S_r) / \sum_{r=1}^{m} \vartheta(S_r) \tag{21}$$

4. Bi-Level Collaborative Optimization Strategy

This paper proposes a bi-level collaborative optimization strategy model based on real-time charging price to guide EV orderly charging and the safe operation of charging stations. The schedulability of EV load is utilized to smooth the load fluctuation of distribution network and ensure its stable operation. As shown in Figure 6, the framework of collaborative optimization strategy is divided into the upper and lower layer, and the upper layer is the EV charging price guidance layer. Firstly, based on the prospect theory, the EV user charging prospect function model considering the influence of price and time factors is established, and the EV load data after the price guidance are transferred to the lower model. The lower layer is the charging station operation layer, which calculates the real-time total load data of the distribution network according to the EV load data, and it takes the voltage fluctuation index and user charging cost as the target under the constraint conditions such as power flow constraint, calculates the real-time price, and updates the price on a rolling basis to guide EV orderly charging.

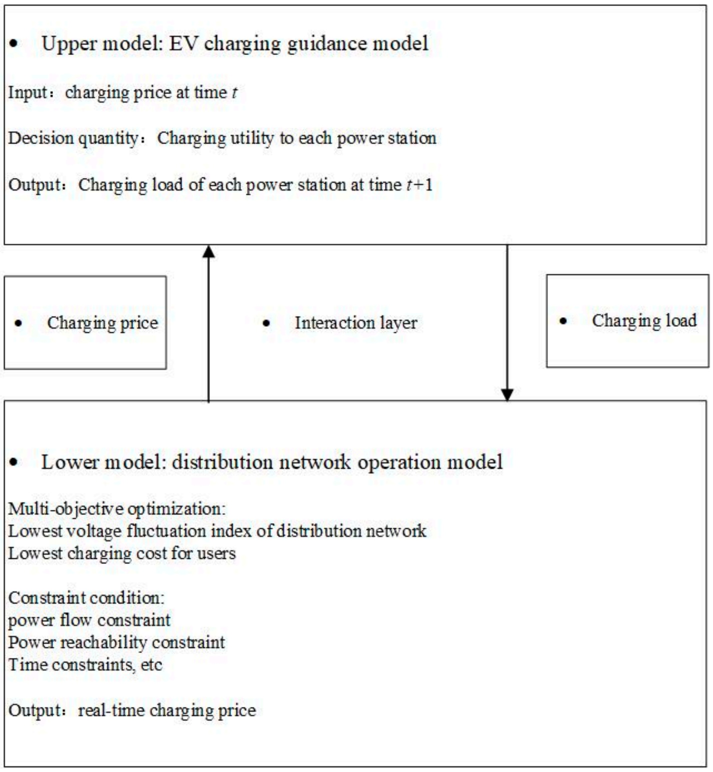

Figure 6. Bi-level collaborative optimization strategy model.

4.1. Objective Function and Constraint Conditions

The purpose of collaborative optimization strategy is to reduce the fluctuation of distribution network and reduce the adverse effects. Therefore, this paper puts forward the voltage fluctuation index to represent the voltage fluctuation of the system. At the same time, considering the economy of EV users, the collaborative optimization strategy is established.

4.1.1. Objective Function

1. Minimum voltage fluctuation index

The primary purpose of collaborative optimization strategy is to alleviate the imbalance of load in the distribution network area and reduce the fluctuation of voltage so as to improve the power quality. In this paper, the voltage fluctuation index is proposed to represent the voltage deviation of regional distribution network system. The voltage deviation of node j at time t can be expressed as:

$$\Delta V_j^t = \left|1 - V_j^t\right| \tag{22}$$

where V_j^t represents the voltage of node j. There are r power grid nodes in the region, so the objective function at time t is the minimum voltage fluctuation index in the region:

$$\partial_{\min} = \min\sum_{j=1}^{r} \Delta V_j^t / r \tag{23}$$

2. Minimum charging cost for users

Users can only respond positively to collaborative optimization strategy when they are profitable, so reducing charging costs for users is undoubtedly one of the goals. Then, the objective function of the charging user n choosing the charging station i can be expressed as

$$U_{\max} = \mathrm{argmax}[U_{ni}] \tag{24}$$

where U_{ni} represents the utility value.

4.1.2. Constraints

1. Income constraints of charging stations

After the charging station operator participates in the price regulation, its profit should not be lower than the profit obtained by the original pricing system so that the operator can be willing to participate in the real-time price strategy.

$$\left(\sum_{k=1}^{m}\sum_{i=1}^{n}\left(SOC_i^g - \mathrm{SOC}_i^r\right)\cdot c_k(t)\right) \geq \sum_{i=1}^{n}\left(\left(\mathrm{SOC}_i^g - SOC_i^r\right)\right)\cdot c_0 \tag{25}$$

In (25), m is the total number of charging stations in the region; n is the total number of EVs to be charged;$c_k(t)$ is the real-time charging price of station k; SOC_i^g is the SOC of EV i after charging; and SOC_i^r is the remaining SOC of EV i at the beginning of charging. c_0 is the unified price before adjustment.

2. Power flow equation constraints

$$\begin{cases} P_{Gi}(t) = V_i(t)\sum\limits_{j=1}^{N} V_j(t)\left(G_{ij}\cos\theta_{ij}(t) + B_{ij}\sin\theta_{ij}(t)\right) + P_{EVi}(t) + P_{oi}(t) \\ Q_{Gi}(t) = V_i(t)\sum\limits_{j=1}^{N} V_j(t)\left(G_{ij}\sin\theta_{ij}(t) - B_{ij}\cos\theta_{ij}(t)\right) + Q_{oi}(t) \end{cases} \tag{26}$$

In (26),$P_{Gi}(t)$ and $Q_{Gi}(t)$ are the active and reactive power injected at node i during time period t, respectively. $P_{oi}(t)$ and $Q_{oi}(t)$ are the conventional active and reactive loads at node i of time period t, respectively, while $P_{EVi}(t)$ represents the charging loads. G_{ij} and B_{ij} are the real and imaginary parts of the node admittance matrix, respectively; $\theta_{ij}(t)$ is the nodal-voltage phase angle difference for the branch ij of time period t; and N is the total number of nodes in the distribution network.

3. Power flow equation constraints

According to the requirements of GB/T12325-2008 "Power Quality and Supply Voltage Deviation", the three-phase supply voltage deviation of 20kV and below should be ±7% of the nominal voltage, which is $0.93 \leq V_i^t \leq 1.07$.

4. Transmission power constraint

$$\begin{cases} P_{ij,t} \leq P_{ij}^{max} \\ Q_{ij,t} \leq Q_{ij}^{max} \end{cases} \tag{27}$$

where P_{ij}^{max} and Q_{ij}^{max} are the upper limits of the active and reactive power that line ij can transmit respectively.

5. Power accessibility constraints

Excessive battery discharge will cause adverse impact to the battery, resulting in charging difficulties and other problems. Therefore, this paper stipulates that the lower limit of the remaining SOC of the EV arriving at the charging station is 10%; thus, the constraint of the power accessibility is

$$SOC_i^{re} \geq 10\% \tag{28}$$

6. Price constraints

The upper limit of the price set by the charging station operator should be lower than the highest psychological expected price of the users to ensure that the EV users can actively participate in the charging guidance, while the lower limit of the price should consider the basic profit of the charging station operator.

$$c_{earn} < c_k(t) < c_{expe} \tag{29}$$

7. Time constraints

Users who choose the fast charging mode have urgent charging needs and cannot wait too long. Therefore, the sum of the user's travel time and time spent in the charging station should be less than $T_{\max}$.

$$T + T' \leq T_{\max} \tag{30}$$

4.2. Analysis of Optimization Calculation Process

The architecture of the strategy proposed in this paper includes the price setting stage and the charging guidance stage, and the simulation process is shown in Figure 7. It mainly includes simulation of EV travel and charging load distribution, calculation of distribution network, and calculation of guided price. The adaptive genetic algorithm (AGA) is adopted for solving. AGA uses a dynamically generated method to determine the probability of adaptive crossover and mutation. In order to maintain the diversity of individual genetics, quickly converge to the global optimum and prevent the genetic algorithm from converging too early to the local optimum.

The adaptive crossover probability P_c and mutation probability P_m can be obtained by the following equation:

$$P_c = \begin{cases} P_{c\_\max} - \left(\frac{P_{c\_\max} - P_{c\_\min}}{M}\right) \times Gen & fit_l > fit_{avg} \\ P_{c\_\max} & fit_l \leq fit_{avg} \end{cases} \tag{31}$$

where $P_{c\_\max}$ is the maximum crossover probability; $P_{c\_\min}$ is the minimum crossover probability; Gen is the current number of iterations; M is the maximum number of iterations;

fit_l indicates the larger fitness in a cross operation; and fit_{avg} represents the average fitness of all individuals in the current iteration.

$$P_m = \begin{cases} P_{m\_\max} - \left(\frac{P_{m\_\max} - P_{m\_\min}}{M}\right) \times Gen & fit_l > fit_{avg} \\ P_{m\_\max} & fit_l \leq fit_{avg} \end{cases} \tag{32}$$

where $P_{m\_\max}$ is the maximum mutation probability; $P_{m\_\min}$ is the minimum mutation probability; Gen is the current iteration number; and M is the maximum number of iterations. fit represents the fitness of the individual in the current mutation operation. Figure 7 shows the operational flowchart of the AGA.

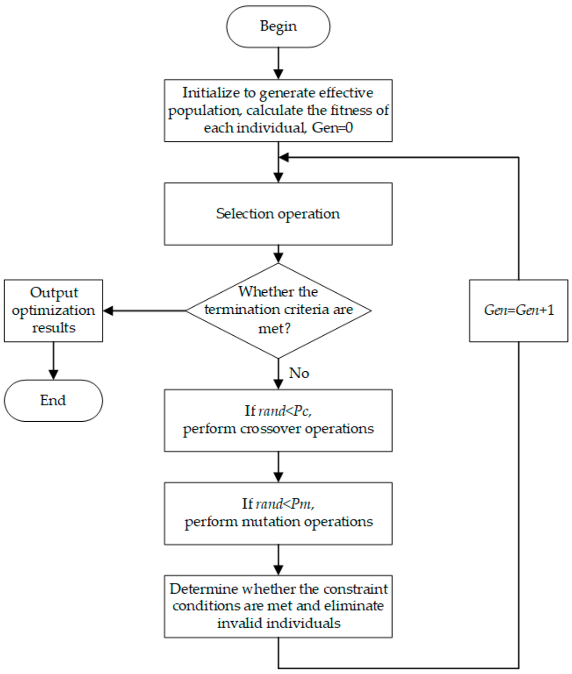

Figure 7. Operational flowchart of the AGA.

- Step 1: Initialize. Generate an effective population and calculate each individual fitness.
- Step 2: Selection operation. N individuals with better fitness are selected and retained. If the optimal fitness meets the set goal or reaches the maximum number of iterations, output the optimal results and stop the operation; otherwise, proceed to the next step.
- Step 3: Crossover operation. When the random variable is less than the adaptive crossover probability, a single point crossover between parents and offspring is performed, resulting in the generation of $2N$ offspring from N parent individuals. The parents and offspring merge to form a new population.
- Step 4: Mutation operation. For a new population, mutation is performed when the random variable is less than the adaptive mutation probability.
- Step 5: Judge the constraint conditions of $3N$ individuals, eliminate the invalid individuals, retain the N individuals with better fitness, return to the second step, and increase the number of iterations once.

This paper sets the specific parameters of the AGA as follows: 70 genetic iterations, a total of 200 individuals in the population. $P_{c\_\max} = 0.9$, $P_{c\_\min} = 0.4$, $P_{m\_\max} = 0.1$, $P_{m\_\min} = 0.01$. The solving process of multi-objective optimization charging strategy is shown in Figure 8, and the specific steps are as follows:

- Initialize EV locations and SOC and import multi-source raw data such as road network, power grid structure, and temperature. Initialize the charging price matrix in time period t, and the simulation takes 15 min as a cycle.

- Each EV travels according to the planned path, and the speed and energy consumption of each road section in time period t are calculated based on the speed-flow model and temperature so as to determine whether the remaining EV power needs to be charged and obtain the spatio-temporal distribution of the charging load.
- Carry out the calculation in the charging station, make statistics on the occupation and queuing of charging piles at each charging station during t period, calculate the power flow of the distribution network, and calculate the queuing time of charging station according to the calculation method of queuing time in literature [15].
- Considering various constraints on the user side and the power grid side, AGA is used to obtain the optimal charging strategy at time t. The steps include population initialization, selection, crossover, mutation, etc.
- According to the optimal solution, the EVs are allocated to the corresponding node for charging.
- Output charging price matrix of 96 periods, user charging cost, and voltage fluctuation index.

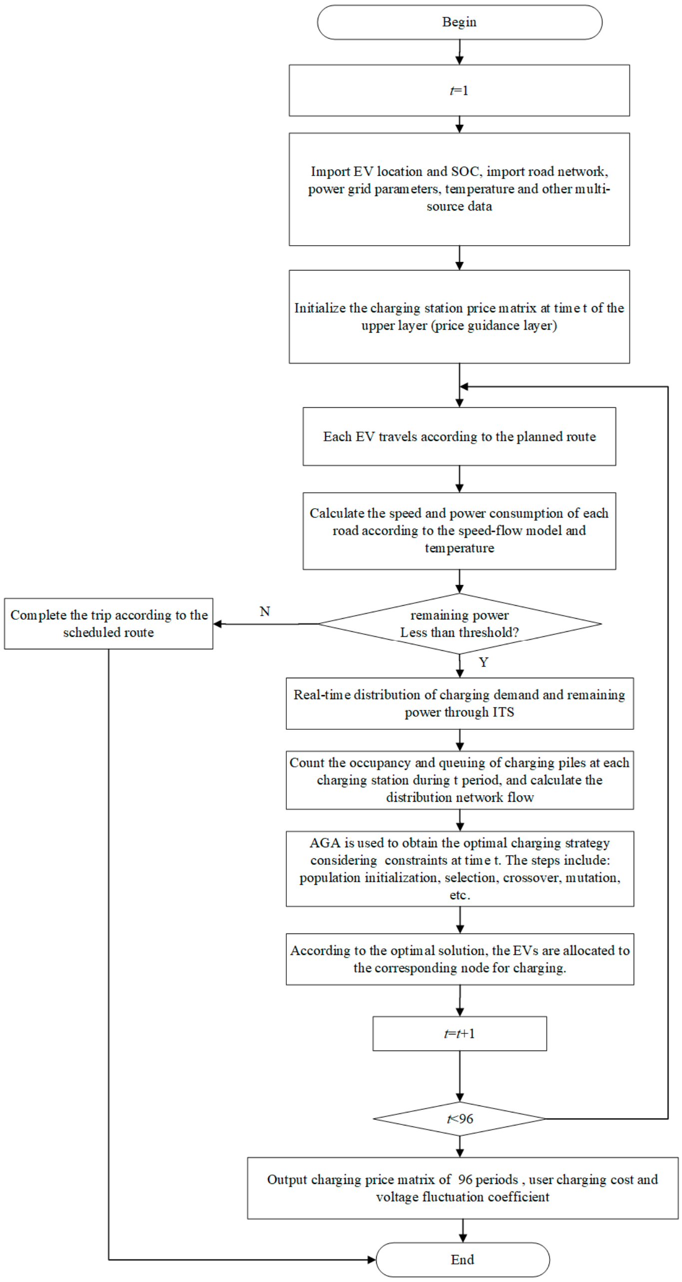

Figure 8. Collaborative optimization strategy calculation process.

5. Results

5.1. Simulation Parameters

Taking the road network in literature [38] as an example, this paper divides the roads in the road network into two levels, in which the values of {a, b, γ} of trunk road are {1.726, 3.15, 3}, and the corresponding values of secondary trunk road are {2.076, 2.870, 3} [39]. Road network parameters and road saturation parameters are given in Table A1 of Appendix A. The road network is coupled with the IEEE 39 node power distribution system. There are 5 fast charging stations in the network, and the number of charging piles in each fast charging station is 10. The ambient temperature is set to 0 °C. The values of other main simulation parameters are shown in Table 1. A total of 1500 EVs participated in the simulation, and the initial time and initial position distribution are shown in Figure A1a,b of Appendix A.

Table 1. Value of main parameters in the simulation.

Parameters	Value	Unit
Charging power	60	kW
Battery capacity	24	kW·h
Disorderly charging price	2.2	$/kW·h
Orderly charging price range	[0.6, 3.5]	$/kW·h
Zero flow velocity	50	km/h

5.2. Analysis of Simulation Results

5.2.1. Analysis of Collaborative Optimization Strategy Results: Power Grid Side

The primary goal of collaborative optimization is to reduce voltage fluctuation and reduce voltage overshoot. This paper takes 15 min as the time period to analyze the improvement effect of adjusting charging price on power quality. The following simulation results are obtained by comparing the collaborative optimization strategy considering user preferences proposed in this paper, the non-preferred charging strategy, and the disorderly charging mode of choosing the nearest charging station without price guidance.

Figures 9a–c and 10a–c show the voltage values of the five charging station nodes and the voltage fluctuation index under the conditions of considering preference, no preference, and disorderly charging.

It can be seen that after the fast charging load is connected, under the disorderly charging strategy, a large number of node voltages are out of limit. The voltage fluctuation of the distribution network is sharp in the three periods of 6:30–8:30, 11:30–14:30, and 17:00–20:00, and the voltage violations occurred 74 times in 42 periods in total. The lowest voltage appears at 12:45 and drops to 0.821 pu. From 17:00 to 20:00, the average drop of node voltage is 10.330%. The voltage fluctuation index rises to 0.143. The maximum voltage fluctuation occurred at 12:30, reaching 0.158.

Under the no-preference charging strategy, the voltage fluctuation index has been improved to some extent, but there are still voltage out of limit occurrences: 16 times in 14 periods, mainly concentrated at 13:15–13:45, 5:00–5:30, and 7:00–7:30. The lowest voltage occurs at 7:45, which is 0.835pu. At 13:15, the voltage fluctuation index reaches 0.0371, which is the peak value. The average voltage fluctuation index is 30.843% lower than that of disorderly charging.

Under the strategy proposed in this paper, the voltage fluctuates between 0.93 and 1.07, and there is no out-of-limit situation. The voltage fluctuation index is between 0.0003 and 0.0203, which is an order of magnitude lower than before. The average voltage fluctuation index is 32.715% lower than that of disorderly charging, which is more effective than the optimization result of non-preference charging strategy.

To sum up, the power flow of the distribution network is changed, and the voltage of each node in the distribution network is affected by adjusting the spatio-temporal access of the fast charge load proposed in this paper. After adjustment, the voltage deviation of the distribution network is reduced, and the power quality is improved to some extent. At the same time, compared with the no-preference charging strategy, the optimization effect of the strategy proposed in this paper is better, the voltage is more stable, and the out-of-limit node is from some to none, which proves that the strategy proposed in this paper is more superior and effective.

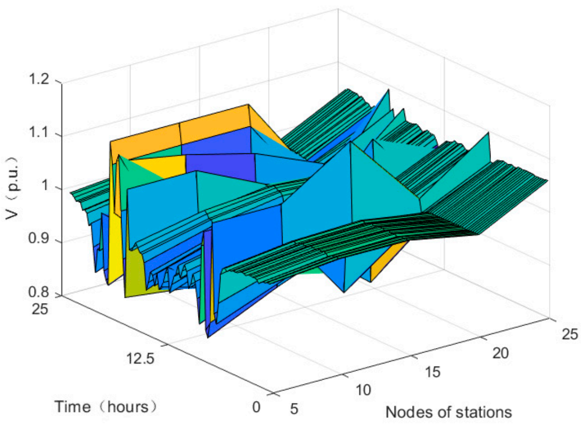

(**a**)

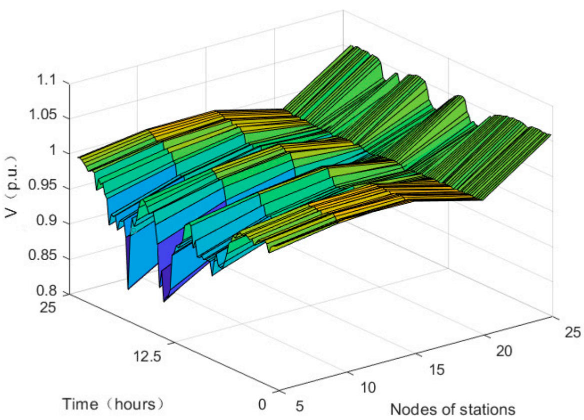

(**b**)

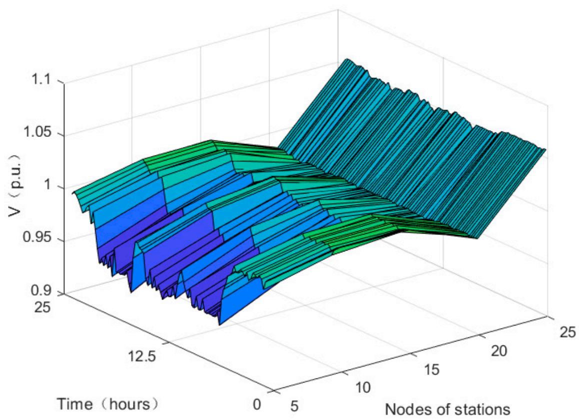

(**c**)

Figure 9. (**a**) Voltage values of stations under disorderly charging strategy; (**b**) Voltage values of stations under non-preferred charging strategy; (**c**) Voltage values of stations under collaborative optimization strategy.

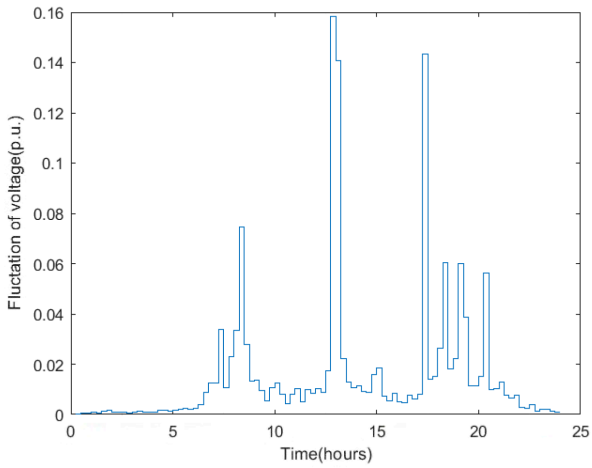

(**a**)

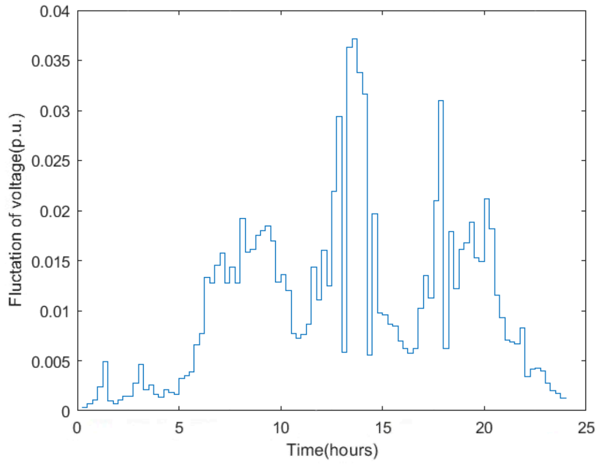

(**b**)

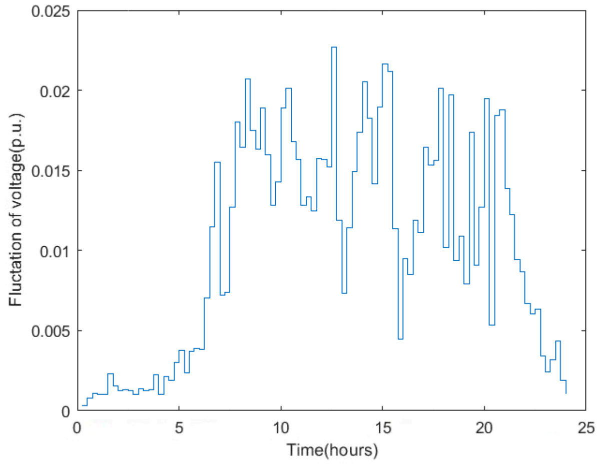

(**c**)

Figure 10. (**a**) Fluctuation index under disorderly charging strategy. (**b**) Fluctuation index under non-preferred charging strategy. (**c**) Fluctuation index under collaborative optimization strategy.

5.2.2. Analysis of Collaborative Optimization Strategy Results: User Side

For EV users, they hope to reduce the charging cost by participating in the optimization strategy, which means the larger utility according to Formula (24). The comparison of utility is shown in Figure 11.

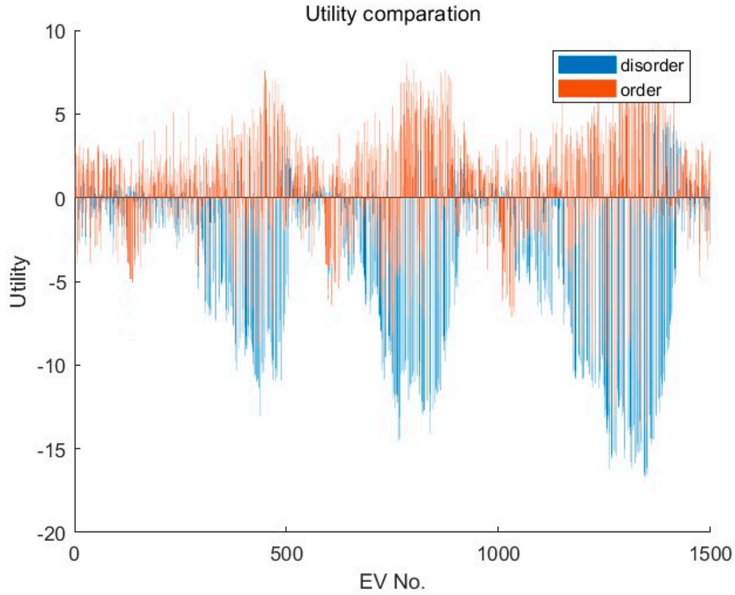

Figure 11. Utility value comparison under orderly and disorderly charging.

Compared with disorderly charging, the collaborative optimization strategy proposed in this paper improves the charging utility value of users by 93.533%, and the average charging utility value increases from −7.832 to 1.916, which means that the charging cost has been effectively reduced. For the majority of charging users, the comprehensive charging cost has been optimized not only in money but also in time.

By responding to the real-time price of different charging stations and accepting guidance and distribution, users can reduce their queuing time and charging costs. In order to simulate the "herding effect" of users in charging decision-making, this paper sets the reference points as time-varying, and the reference points of price, queue time, and travel time are shown in the Figure 12a–c.

The objective weight of each attribute is mined through fuzzy clustering. The clustering results under partial confidence degree are as follows:

- $0.65 < F_k \leq 0.70$, all samples are divided into 1 cluster when no attribute is deleted, 2 clusters when price attribute is deleted, and 1 cluster when time attribute is deleted.
- $0.70 < F_k \leq 0.75$, all samples are divided into 2 clusters when no attribute is deleted, 8 clusters when price attribute is deleted, and 3 clusters when time attribute is deleted.
- $0.75 < F_k \leq 0.80$, all samples are divided into 5 clusters when no attribute is deleted, 68 clusters when price attribute is deleted, and 20 clusters when time attribute is deleted.
- $0.80 < F_k \leq 0.85$, all samples are divided into 7 clusters when no attribute is deleted, 117 clusters when price attribute is deleted, and 40 clusters when time attribute is deleted.
- $0.85 < F_k \leq 0.90$, all samples are divided into 11 clusters when no attribute is deleted, 138 clusters when price attribute is deleted, and 49 clusters when time attribute is deleted.
- $0.90 < F_k \leq 0.95$, all samples are divided into 19 clusters when no attribute is deleted, 141 clusters when price attribute is deleted, and 51 clusters when time attribute is deleted.
- $0.95 < F_k \leq 1.00$, all samples are divided into 23 clusters when no attribute is deleted, 144 clusters when price attribute is deleted, and 52 clusters when time attribute is deleted.

According to the definition of attribute importance, the weight of each attribute is assigned as $(C, T, T') = (0.2298, 0.3851, 0.3851)$.

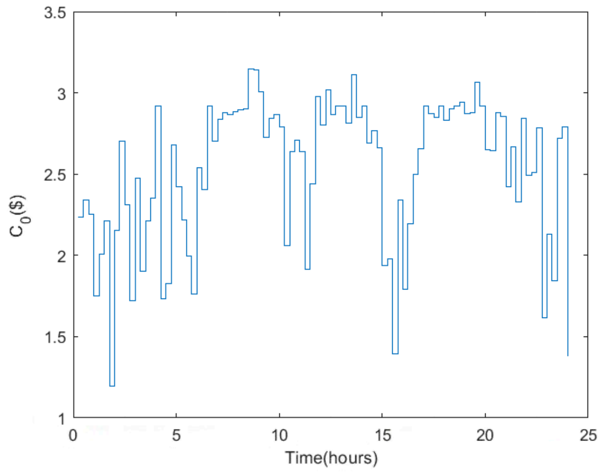

(**a**)

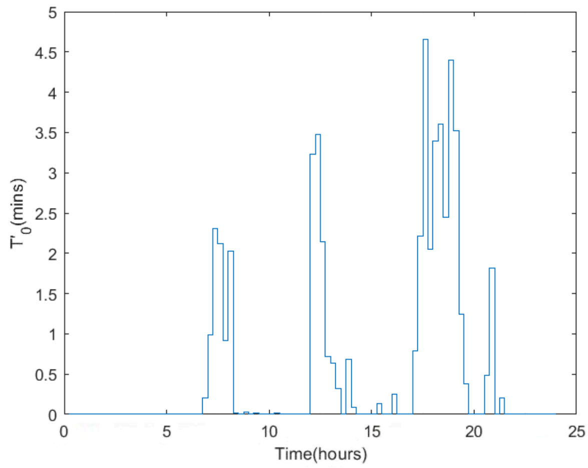

(**b**)

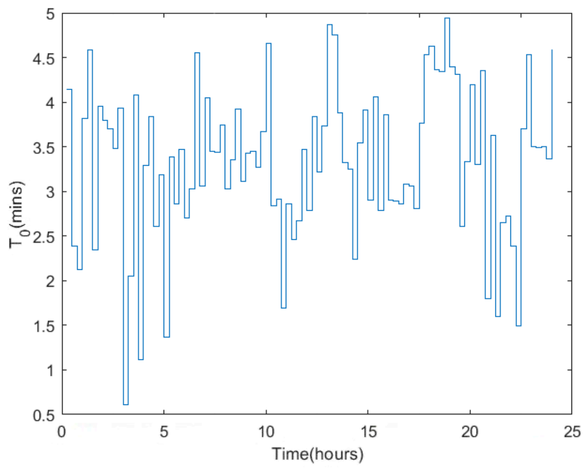

(**c**)

Figure 12. (**a**) Reference point of price; (**b**) Reference point of queue time; (**c**) Reference point of travel time.

5.2.3. Analysis of Collaborative Optimization Strategy Results: Station Side

From the point of view of charging stations, through reasonable pricing and orderly guidance, EVs can be dynamically allocated to reduce congestion in charging stations and improve the rationality of charging station utilization.

The load of each charging station before and after optimization is shown in Figure 13a,b. It can be seen that the load of node 5 is too large in some time periods under disorderly charging, and the voltage has exceeded the limit for many times. However, after orderly guidance, the load of node 5 is significantly reduced and transferred to other nodes, which proves the effectiveness of the collaborative optimization in this paper.

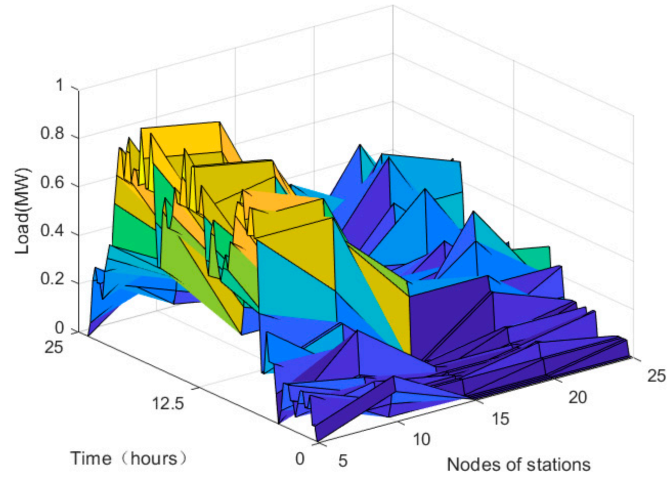

(**a**)

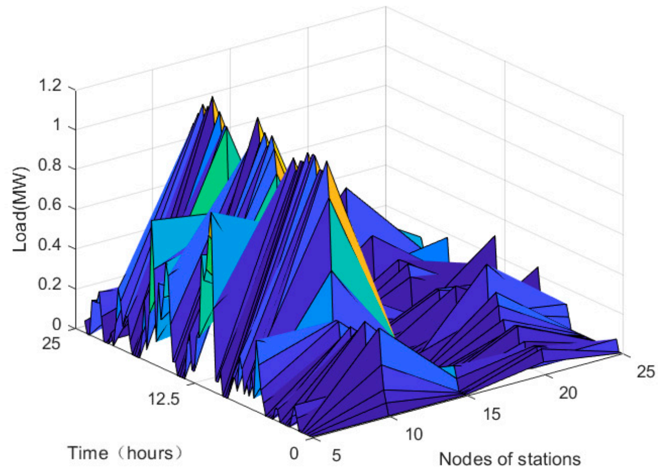

(**b**)

Figure 13. (**a**) Disorderly load without optimization; (**b**) Orderly load with optimization.

In this paper, three scenarios under 0 °C, 25°C, and −20 °C are selected, respectively, for comparative analysis of queuing time. Among them, the charging efficiency under −20 °C is 80%, and the charging efficiency under 0 °C and 25 °C is 98%. The comparison of queuing time at different temperatures is shown in Figure 14. The number of queuing vehicles and the average queuing time are given in Table 2.

Table 2. Queueing conditions at different temperatures.

Temperature	**−20 °C**		**0 °C**		**25 °C**	
Charging Strategy	**Disorderly**	**Orderly**	**Disorderly**	**Orderly**	**Disorderly**	**Orderly**
Number of queueing EVs	480	252	415	159	442	202
Average queue time	12.635	7.471	6.649	4.202	5.725	3. 397

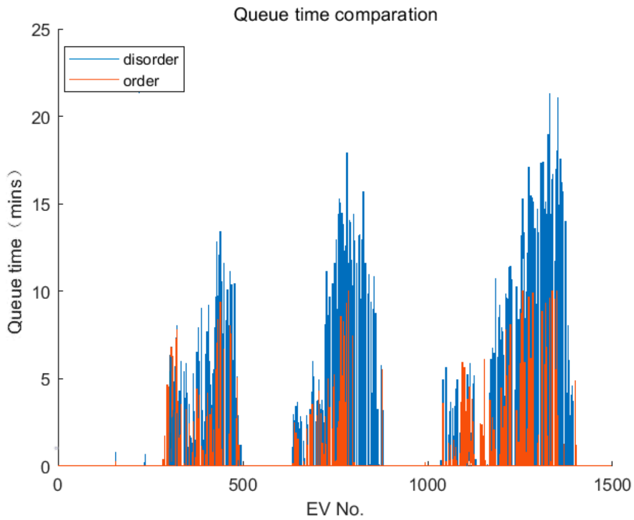

(**a**)

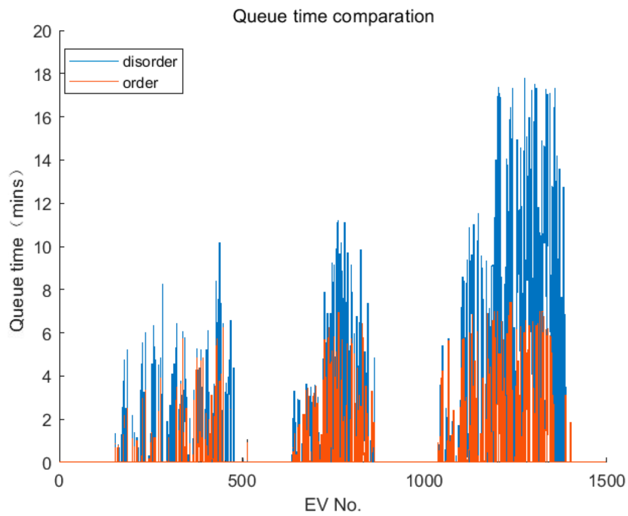

(**b**)

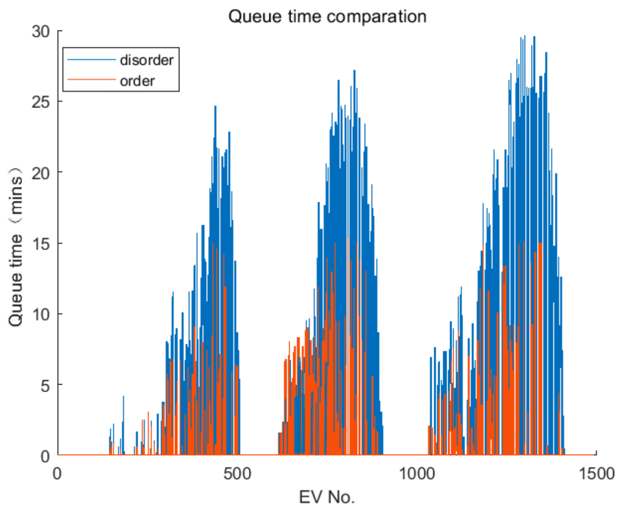

(**c**)

Figure 14. (**a**) Queue time comparison at 0 °C. (**b**) Queue time comparison at 25 °C. (**c**) Queue time comparison at −20 °C.

By analyzing the number of queueing EVs and the average queue time data in Figure 11 and comparing the data in Table 1 at different temperatures, it can be concluded that, compared to disorderly charging, the average queue time at −20 °C, 0 °C, 25 °C decreased by 40.870%, 36.802%, and 40.663%, respectively, and the number of queueing EVs decreased by 47.916%, 61.686%, and 54.298%, respectively. The results show that dynamic pricing can not only improve the congestion inside the charging stations but also effectively distribute the charging pressure to other stations. At −20 °C, the relative SOC decreases, and the charging efficiency decreases, and the heating of the AC system accelerates the power consumption speed, so the remaining power of EV is lower and the charging time is longer, leading to the increase in the queuing time. The average queue time in the three scenarios is significantly reduced, which verifies the validity of the pricing strategy proposed in this paper.

In addition, optimization strategy and reasonable pricing can effectively balance the load among charging stations, reduce congestion within stations, and improve the comprehensive utilization rate of each charging station; thus, it has not reduced the profits of charging station operators, which represents the electricity sales profits of all charging stations during the 96 periods. The total profit of charging stations under the pricing strategy in this paper is USD 30,975.816, while that under the original fixed charging pricing strategy is USD 30,565.499. The profit comparison of charging stations is shown in Figure 15.

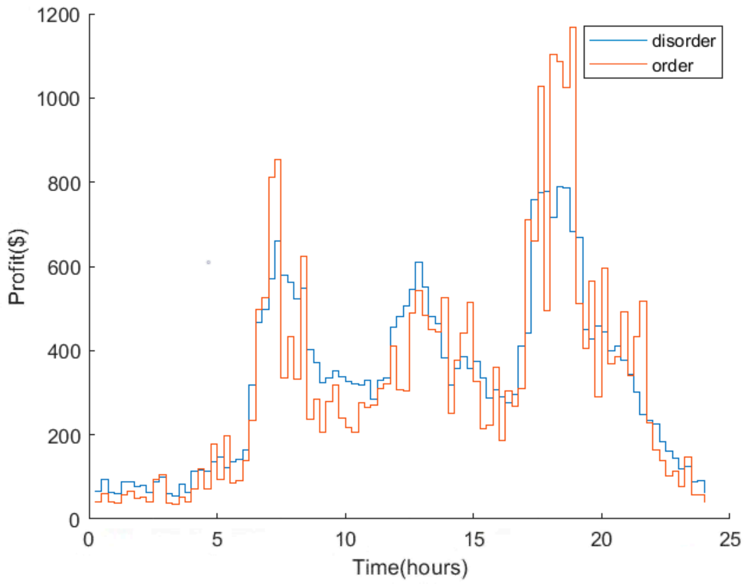

Figure 15. Profit comparison.

To sum up, the strategy proposed in this paper guides users through price leverage; the charging behavior is dynamically adjusted according to the initial load of the distribution network, and the spatial distribution changes of the fast charging EVs access in different periods has a good regulating effect. From the perspective of the power grid, it can significantly reduce the number of distribution network voltage threshold nodes and improve the power quality of the distribution network. From the perspective of user groups, the charging cost is effectively reduced, and the queuing time of users is greatly reduced. The irrational charging decision model and time-varying reference point constructed considering user preferences can fully stimulate the response potential of users. From the point of view of charging stations, the utilization rate of charging stations is improved, so the profit space of charging station operators is not reduced.

Figure 16 shows the convergence analysis curve of the optimization algorithm proposed in this article. After approximately 50 iterations, the optimal solution was obtained, proving that AGA has good convergence.

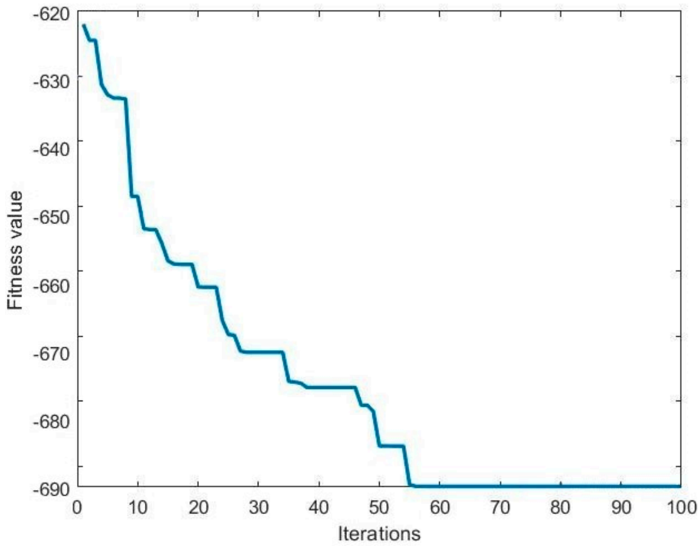

Figure 16. Convergence analysis.

6. Discussion

This paper proposes a collaborative optimization strategy considering psychological preference. By adjusting the real-time charging price to guide the charging decision behavior of users, it can change the spatio-temporal distribution of charging load, optimize the power quality of distribution network, effectively reduce the charging cost of EV users, and ensure the overall benefit of charging station operators. It is significant for suppressing load fluctuation, maintaining power grid stability and economic operation. Specific conclusions are as follows:

(1) The spatio-temporal prediction of charging load considering speed-temperature proposed in this paper considers road constraints, practical speed–flow relationship model, and temperature, and simulates the driving conditions and the remaining SOC of EVs in the urban road network so as to obtain the spatio-temporal distribution of charging load by coupling the regional distribution network.

(2) This paper proposes a charging decision model based on the irrational psychology and decision-making behavior of users, and on this basis combines fuzzy clustering with the relative positive domain theory of rough set to mine the attribute preference, obtaining a multi-attribute charging decision model that considers the user's psychological preference. The charging decision-making model formulated by this method is more in line with the decision-making process of the user, and the collaborative optimization strategy formulated based on this can effectively stimulate the user's responsiveness.

(3) A bi-level collaborative optimization strategy model is proposed. By changing the price of each power station to guide users charging in an orderly manner, the average voltage fluctuation index is reduced by 32.715%, the voltage out-of-limit situation is solved, and the average charging utility value of users in the region is increased from −7.832 to 1.916, effectively reducing the charging cost of users. At the same time, the congestion of charging stations has been alleviated, and the profit of charging stations has not been affected.

To sum up, the strategy proposed in this paper can satisfy the needs of EVs, fast charging stations, and distribution networks. With the development and improvement of the charging market in the future, the EV-station-grid will face competition and cooperation, and the interaction between the three parties will lead to more complex charging decision-making scenarios with the game and V2G. It will be the focus of future research to develop incentive and control strategies for user charging behavior in multiple scenarios.

Author Contributions: Conceptualization, C.W. and S.M.; methodology, C.W.; software, C.W.; validation, C.W., Q.W. and Y.D.; formal analysis, N.Y.; investigation, Z.C.; resources, S.M.; data curation, C.W.; writing—original draft preparation, C.W.; writing—review and editing, S.M.; visualization, C.W.; supervision, S.M.; project administration, Q.W.; funding acquisition, None. All authors have read and agreed to the published version of the manuscript.

Funding: This research received no external funding.

Data Availability Statement: The data presented in this study are available on request from the corresponding author.

Conflicts of Interest: The authors declare no conflict of interest.

Appendix A

Table A1. Road network parameters and saturation parameters.

Nodes	Nodes	Distance	Grade	6:30–8:30	8:30–11:30	11:30–13:30	13:30–17:00	17:00–19:00	19:00–23:00	Other Time
1	2	1.71	II	0.5	0.3	0.4	0.3	0.5	0.3	0.2
1	5	2.704	II	0.55	0.3	0.4	0.3	0.55	0.3	0.2
2	3	1.126	II	0.55	0.3	0.4	0.3	0.55	0.3	0.2
2	4	3.39	II	0.6	0.35	0.4	0.35	0.6	0.3	0.25
3	4	1.552	II	0.6	0.35	0.4	0.35	0.6	0.3	0.25
3	9	1.986	II	0.55	0.3	0.4	0.3	0.55	0.3	0.2
9	4	1.613	II	0.6	0.35	0.4	0.35	0.6	0.3	0.25
9	8	1.805	II	0.55	0.3	0.4	0.3	0.55	0.3	0.2
9	10	2.137	II	0.6	0.35	0.4	0.35	0.6	0.3	0.25
10	8	1.557	I	0.65	0.35	0.45	0.35	0.65	0.35	0.3
10	13	1.924	II	0.65	0.35	0.45	0.35	0.65	0.35	0.3
10	14	1.017	II	0.6	0.35	0.4	0.35	0.6	0.3	0.25
14	13	0.747	II	0.7	0.35	0.45	0.35	0.7	0.35	0.3
14	19	1.037	I	0.55	0.3	0.4	0.3	0.55	0.35	0.3
14	21	1.687	I	0.7	0.4	0.5	0.4	0.7	0.4	0.3
14	22	0.926	I	0.75	0.45	0.5	0.45	0.75	0.45	0.3
22	23	1.429	II	0.55	0.3	0.4	0.3	0.55	0.35	0.3
23	24	0.878	I	0.75	0.45	0.5	0.45	0.75	0.45	0.3
24	25	0.794	II	0.5	0.3	0.4	0.3	0.5	0.3	0.2
21	20	1.3	I	0.6	0.35	0.4	0.35	0.6	0.3	0.25
20	19	1.126	II	0.55	0.3	0.4	0.3	0.55	0.3	0.2
20	18	0.87	II	0.5	0.3	0.4	0.3	0.5	0.3	0.2
18	17	2.149	II	0.55	0.3	0.4	0.3	0.55	0.3	0.2
17	19	1.271	II	0.6	0.35	0.4	0.35	0.6	0.3	0.25
19	13	1.686	II	0.5	0.3	0.4	0.3	0.5	0.3	0.2
13	8	1.843	I	0.75	0.45	0.5	0.45	0.75	0.45	0.3
13	11	2.387	I	0.75	0.45	0.5	0.45	0.75	0.45	0.3
8	4	1.5	II	0.55	0.3	0.4	0.3	0.55	0.3	0.2
8	7	2.763	II	0.55	0.3	0.35	0.3	0.55	0.25	0.2
8	11	1.836	II	0.7	0.35	0.45	0.35	0.7	0.35	0.3
11	7	1.986	II	0.55	0.3	0.35	0.3	0.55	0.25	0.2
11	12	1.162	II	0.7	0.35	0.45	0.35	0.7	0.35	0.3
11	16	1.801	II	0.55	0.3	0.35	0.3	0.55	0.25	0.2
16	17	1.76	II	0.7	0.35	0.45	0.35	0.7	0.35	0.3
16	12	1.334	II	0.55	0.3	0.35	0.3	0.55	0.25	0.2
16	15	2.634	I	0.75	0.45	0.5	0.45	0.75	0.45	0.3
15	12	1.413	I	0.75	0.45	0.5	0.45	0.75	0.45	0.3
12	7	0.739	II	0.7	0.35	0.45	0.35	0.7	0.35	0.3
7	6	2.134	I	0.65	0.7	0.7	0.65	0.65	0.6	0.2
7	4	1.023	I	0.65	0.7	0.7	0.65	0.65	0.6	0.2
7	5	1.35	I	0.65	0.7	0.7	0.65	0.65	0.6	0.2
5	6	0.859	I	0.6	0.75	0.8	0.75	0.6	0.6	0.2

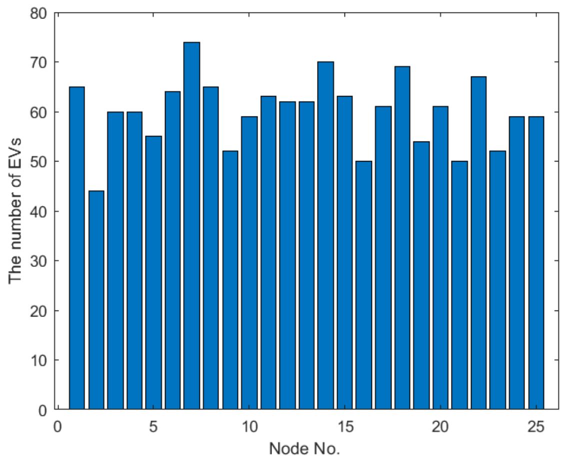

(**a**)

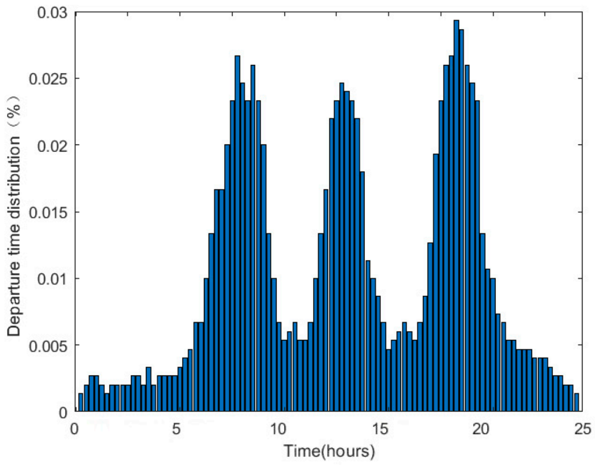

(**b**)

Figure A1. (**a**) Initial position distribution of EVs; (**b**) Departure time distribution of EVs.

References

1. Zhang, S.; Wang, D.; Cheng, H. Key Technologies and Challenges of Low-carbon Integrated Energy System Planning for Carbon Emission Peak and Carbon Neutrality. *Autom. Electr. Power Syst.* **2022**, *46*, 189–207. [CrossRef]
2. Duan, X.; Hu, Z.; Song, Y.; Strunz, K.; Cui, Y.; Liu, L. Planning Strategy for an Electric Vehicle Fast Charging Service Provider in a Competitive Environment. *IEEE Trans. Transp. Electrif.* **2022**, *8*, 3056–3067. [CrossRef]
3. Shi, X.; Xu, Y.; Guo, Q.; Sun, H. Optimal Dispatch Based on Aggregated Operation Region of EV Considering Spatio-Temporal Distribution. *IEEE Trans. Sustain. Energy* **2022**, *13*, 715–731. [CrossRef]
4. Xu, S.; Zhang, H.; Shi, D.; Guo, X.; Lin, X.; Li, Z. Setting Strategy of Charging Service Fee for Fast Charging Load of Smart Cities. *Proc. CSEE* **2020**, *40*, 14.
5. Bayram, I.S.; Tajer, A.; Abdallah, M.; Qaraqe, K. Capacity Planning Frameworks for Electric Vehicle Charging Stations with Multiclass Customers. *IEEE Trans. Smart Grid* **2015**, *6*, 1934–1943. [CrossRef]
6. Darii, N.; Turri, R.; Sunderland, K.; Bignucolo, F. A Novel Unidirectional Smart Charging Management Algorithm for Electric Buses. *Electronics* **2023**, *12*, 852. [CrossRef]
7. Alvarez Guerrero, J.D.; Bhattarai, B.; Shrestha, R.; Acker, T.L.; Castro, R. Integrating Electric Vehicles into Power System Operation Production Cost Models. *World Electr. Veh. J.* **2021**, *12*, 263. [CrossRef]
8. Yang, J.; Gou, F.J.; Huang, Y.; He, Z.Y. Residential Area Electric Vehicle Charging Pricing Strategy Based on Uncertainty Measure. *Power Syst. Technol.* **2018**, *42*, 105–111.
9. Sonmez, M.A.; Bagriyanik, M. A Novel Priority-Based Load Management Method that Improves Comfort in Residential Demand Response. *Arab. J. Sci. Eng.* **2022**, *47*, 2763–2779. [CrossRef]
10. Chen, L.; Pan, Z.; Yu, T. Real-time Optimal Dispatch for Large-scale Electric Vehicles Based on Dynamic Non-cooperative Game Theory. *Autom. Electr. Power Syst.* **2019**, *43*, 32–40. [CrossRef]
11. Rehman, U.U. A Decentralized Dynamic Marketing-Based Demand Response Using Electric Vehicles in Smart Grid. *Arab. J. Sci. Eng.* **2020**, *45*, 6475–6488. [CrossRef]

12. Yang, H.; Xie, X.; Vasilakos, A.V. Noncooperative and Cooperative Optimization of Electric Vehicle Charging Under Demand Uncertainty: A Robust Stackelberg Game. *IEEE Trans. Veh. Technol.* **2016**, *65*, 1043–1058. [CrossRef]
13. Mao, D.; Huang, X.; Chen, Z.; Lv, Y.; Tian, J.; Yang, Z. Load Transfer Path Search and Its Evaluation between Networks in Consideration of the Mobile Energy Storage of Electric Vehicles. *World Electr. Veh. J.* **2021**, *12*, 210. [CrossRef]
14. Li, Y.; Liu, X.; Wen, F.; Zhang, X.; Wang, L.; Xue, Y. Dynamic Charging Scheduling for Electric Vehicles Considering Real-Time Traffic Flow. In Proceedings of the 2018 IEEE Power & Energy Society General Meeting (PESGM), Portland, OR, USA, 5–10 August 2018; pp. 1–5. [CrossRef]
15. Shao, Y.; Mu, Y.; Lin, J.; Wang, K.; Gong, Y. Fast Charging Guidance Strategy for Multiple Demands of Electric Vehicle, Fast Charging Station and Distribution Network. *Autom. Electr. Power Syst.* **2019**, *43*, 60–66. [CrossRef]
16. Timotheus, K.; Carlos, N.J. Abstract argumentation and the rational man. *J. Log. Comput.* **2021**, *31*, 654–699.
17. Zhou, S. An Empirical Study on the Impact of Herd Effect of China's Open-ended Stock Fund on Stock Market Volatility. In Proceedings of the 2021 17th International Conference on Computational Intelligence and Security (CIS), Chengdu, China, 19–22 November 2021; pp. 556–559. [CrossRef]
18. Liu, J.; Wang, W.; Li, D.; Wan, S.; Liu, H. Role of Gifts in Decision Making: An Endowment Effect Incentive Mechanism for Offloading in the IoV. *IEEE Internet Things J.* **2019**, *6*, 6933–6951. [CrossRef]
19. Zahir, S. Geometry of decision making and the vector space formulation of the analytic hierarchy process. *Eur. J. Oper. Res.* **1999**, *112*, 373–396. [CrossRef]
20. Xu, X.; Chen, X. Research of a kind of method of multi-attributes and multi-schemes large group decision making. *J. Syst. Eng.* **2008**, *23*, 137–141.
21. Xu, X.; Chen, X.; Tang, H. A kind of large valued preference group decision making method oriented utility information. *Control. Decis.* **2009**, *24*, 440–445+450. [CrossRef]
22. Nie, R.-X.; Wang, J.-Q. Prospect Theory-Based Consistency Recovery Strategies with Multiplicative Probabilistic Linguistic Preference Relations in Managing Group Decision Making. *Arab. J. Sci. Eng.* **2020**, *45*, 2113–2130. [CrossRef]
23. Chicco, G.; Napoli, R.; Piglione, F. Comparisons Among Clustering Techniques for Electricity Customer Classification. *IEEE Trans. Power Syst.* **2006**, *21*, 933–940. [CrossRef]
24. Liu, X.; Pedrycz, W.; Chai, T.; Song, M. The Development of Fuzzy Rough Sets with the Use of Structures and Algebras of Axiomatic Fuzzy Sets. *IEEE Trans. Knowl. Data Eng.* **2009**, *21*, 443–462. [CrossRef]
25. Zhang, T.; Li, Z.; Ma, F. Improved Rough Fuzzy K-means Clustering based on Imbalanced Measure of Cluster Sizes. *Inf. Control.* **2020**, *49*, 281–288. [CrossRef]
26. Arslan, H. A Parallel Fully Dynamic Iterative Bio-Inspired Shortest Path Algorithm. *Arab. J. Sci. Eng.* **2020**, *45*, 10115–10130. [CrossRef]
27. Salamanis, A.; Kehagias, D.D.; Filelis-Papadopoulos, C.K.; Tzovaras, D.; Gravvanis, G.A. Managing Spatial Graph Dependencies in Large Volumes of Traffic Data for Travel-Time Prediction. *IEEE Trans. Intell. Transp. Syst.* **2016**, *17*, 1678–1687. [CrossRef]
28. Shao, Y.; Mu, Y.; Yu, X.; Dong, X.; Jia, H.; Wu, J.; Zeng, Y. A Spatial-temporal Charging Load Forecast and Impact Analysis Method for Distribution Network Using EVs-Traffic-Distribution Model. *Proc. CSEE* **2017**, *37*, 13. [CrossRef]
29. Wang, H.; Zhang, M.; Yang, X. Electric vehicle charging demand forecasting based on influence of weather and temperature. *Electr. Meas. Instrum.* **2017**, *54*, 123–128.
30. Yao, E.; Wang, M.; Song, Y.; Yang, Y. State of Charge Estimation Based on Microscopic Driving Parameters for Electric Vehicle's Battery. *Math. Probl. Eng.* **2013**, *2013*, 946747. [CrossRef]
31. Mazumdar, T.; Raj, S.P.; Sinha, I. Reference price research: Review and Propositions. *J. Mark.* **2005**, *69*, 84–102. [CrossRef]
32. Chen, L.; Yang, F.; Jiang, H.; Li, H. A Study of Travel Choice Behavior Based on Mental Accounting. *J. Shanghai Jiaotong Univ.* **2016**, *50*, 7. [CrossRef]
33. Chen, X.; Wang, H.; Wu, F.; Wu, Y.; Gonzalez, M.C.; Zhang, J. Multimicrogrid Load Balancing Through EV Charging Networks. *IEEE Internet Things J.* **2022**, *9*, 5019–5026. [CrossRef]
34. Luo, Y.; Feng, G.; Wan, S.; Zhang, S.; Li, V.; Kong, W. Charging scheduling strategy for different electric vehicles with optimization for convenience of drivers, performance of transport system and distribution network. *Energy* **2020**, *194*, 116807. [CrossRef]
35. Visaria, A.A.; Jensen, A.F.; Thorhauge, M.; Mabit, S.E. User preferences for EV charging, pricing schemes, and charging infrastructure. *Transp. Res. Part A Policy Pract.* **2022**, *165*, 120–143. [CrossRef]
36. Wang, C.; Ma, S.; Cai, Z.; Yan, N.; Wang, Q. Bounded rational real-time charging pricing strategy under the traffic-grid coupling network. *IET Electr. Syst. Transp.* **2022**, *12*, 251–268. [CrossRef]
37. Yang, X.; Niu, D.; Sun, L.; Ji, Z.; Zhou, J.; Wang, K.; Siqin, Z. A bi-level optimization model for electric vehicle charging strategy based on regional grid load following. *J. Clean. Prod.* **2021**, *325*, 129313. [CrossRef]
38. Hodgson, M.J. A Flow-Capturing Location-Allocation Model. *Geogr. Anal.* **1990**, *22*, 270–279. [CrossRef]
39. Zhang, M.; Sun, Q.; Yang, X. Electric Vehicle Charging Load Prediction Considering Multi-source Information Real-time Interaction and User Regret Psychology. *Power Syst. Technol.* **2022**, *46*, 632–641.